Biochimica et Biophysica Acta 1833 (2013) 712–722

Contents lists available at SciVerse ScienceDirect

Biochimica et Biophysica Acta

journal homepage: www.elsevier.com/locate/bbamcr

Membrane tension homeostasis of epithelial cells through surface area regulation in response to osmotic stress

Anna Pietuch, Bastian R. Brückner, Andreas Janshoff *

Institute of Physical Chemistry, Georg-August-University of Goettingen, Tammannstrasse 6, 37077 Goettingen, Germany

ARTICLE INFO

Article history:
Received 14 September 2012
Received in revised form 2 November 2012
Accepted 7 November 2012
Available online 23 November 2012

Keywords:
Osmotic stress
Epithelial cell
Atomic force microscopy
Membrane tension
Surface area regulation
Microvilli

ABSTRACT

Osmotic stress poses one of the most fundamental challenges to living cells. Particularly, the largely inextensible plasma membrane of eukaryotic cells easily ruptures under in-plane tension calling for sophisticated strategies to readily respond to osmotic stress. We describe how epithelial cells react and adapt mechanically to the exposure to hypotonic and hypertonic solutions in the context of a confluent monolayer. Site-specific indentation experiments in conjunction with tether pulling on individual cells have been carried out with an atomic force microscope to reveal spatio-temporal changes in membrane tension and surface area. We found that cells compensate for an increase in lateral tension due to hypoosmotic stress by sacrificing excess of membrane area stored in protrusions and invaginations such as microvilli and caveolae. At mild hypotonic conditions lateral tension increases partly compensated by surface are regulation, i.e. the cell sacrifices some of its membrane reservoirs. A loss of membrane–actin contacts occurs upon exposure to stronger hypotonic solutions giving rise to a drop in lateral tension. Tension release recovers on longer time scales by an increasing endocytosis, which efficiently removes excess membrane from the apical side to restore the initial pre-stress. Hypertonic solutions lead to shrinkage of cells and collapse of the apical membrane onto the cortex. Exposure to distilled water leads to stiffening of cells due to removal of excess surface area and tension increase due to elevated osmotic pressure across the plasma membrane.

1. Introduction

The plasma membrane of cells is a highly dynamic and strongly regulated two-dimensional liquid crystal. Many cellular processes like endo- and exocytosis [1,2], cell migration [3], cell spreading [4,5] and mitosis [6] are regulated by an intrinsic feature of the plasma membrane, the membrane tension. The plasma membrane tension encompasses the in-plane tension of the lipid bilayer, and the membrane–cytoskeleton adhesion, which is actively controlled by the contractile actomyosin cortex [7]. The intricate interplay between the plasma membrane and its cortex enables cells to withstand mechanical challenges posed by the environment. Considering that membranes are thin and fragile structures sophisticated feedback circuits are necessary based on tension homeostasis to maintain an intact shell. Osmotic stress is a physiologically relevant mechanical stimulus since animal cells have to sustain substantial fluctuations in the osmolarity of external fluids, which produces considerable pressure differences between the cytosol and the environment. Osmotic pressure forces the cell to quickly adapt in order to avoid damages of the largely inextensible plasma membrane. When cells are subjected to a hypoosmotic solution they increase their volume due to influx of water and subsequently they extend their projected surface area. Groulx et al. reported that animal cells can increase their surface area by a factor of 3 and 10 times their volume depending on the cell type [8]. As membranes cannot bear large strains (3–4%), they require regulatory processes to maintain the overall plasma membrane tension below lysis tension; more precisely, tension driven surface area regulation is necessary to accommodate changes in tension. Concretely, high tension is buffered by an excess of membrane area, while a decrease in membrane area is triggered if the tension lowers [9]. To provide sufficient membrane area, cells store excess membrane in reservoirs like microvilli and caveolae, which by virtue of unfolding can buffer membrane tension. Kozera and coworkers showed that caveolae might act as membrane reservoirs to compensate for an increase in membrane tension induced by swelling [10]. So far, a comprehensive picture of membrane homeostasis is lacking since it is difficult to measure surface area and tension simultaneously to confirm the regulative relationship between the two parameters. In this study, we use a unique combination of site-specific indentation followed by tether pulling to acquire tension and excess area of the apical side of epithelial cells spatio-temporally resolved. Polar epithelial cells as those from the intestine or kidney are suitable candidates to study the impact of environmental physicochemical stimuli on changes in membrane tension since they frequently face changes in the chemical potential. Here, we

* Corresponding author. Tel.: +49 551 39 10663; fax: +49 551 39 14411.
E-mail addresses: apietuc@gwdg.de (A. Pietuch), b.r.brueckner@chemie.uni-goettingen.de (B.R. Brückner), ajansho@gwdg.de (A. Janshoff).

0167-4889/$ – see front matter © 2012 Elsevier B.V. All rights reserved.
http://dx.doi.org/10.1016/j.bbamcr.2012.11.006

used Madin Darby canine kidney cells (MDCK II) grown to confluence and challenged by different osmotic solutions to investigate the mechanical response of the plasma membrane with respect to tension-buffering membrane reservoirs. Therefore, indentation experiments, analyzed with an extended liquid droplet model for adherent cells, were carried out with an atomic force microscope (AFM) to simultaneously assess local changes in membrane tension and at the same time and location to monitor the excess membrane area as a function of osmotic pressure. The latter task is achieved by measuring the apparent area modulus of the plasma membrane mirroring the amount of stored excess area. In conjunction with membrane tether pulling experiments, as an independent mechanical approach, we were able to show how epithelial cells adjust their surface area in response to tension changes. Furthermore, we monitored morphological changes due to cell swelling and shrinking showing distinct alteration in tension buffering membrane reservoirs such as microvilli. We found that MDCK II cells sacrifice their microvilli to generate excess membrane readily consumed to accommodate rising tension. Lysis of the plasma membrane is prevented by loosening membrane–actin links and sacrificing membrane reservoirs. However, exposure to distilled water exhausts all existing reservoir and consequently leads to lysis. Long-term monitoring of tension and surface area reveals that membrane tension largely recovers at the expense of membrane area taken-up via an increased endocytosis rate.

2. Materials and methods

2.1. Cell culture

MDCK II cells, obtained from the Health Protection Agency, Salisbury, UK, were maintained in minimal essential medium (MEM) with Earle's salts and 2.2 g/L $NaHCO_3$ (Biochrom, Berlin, Germany) supplemented with 4 mM L-glutamine, penicillin–streptomycin and 10% FCS at 37 °C in a 7.5% CO_2 humidified incubator. Confluent cells were released with trypsin/EDTA (0.5%/0.2%) (Biochrom, Berlin, Germany) and subcultured weekly.

2.2. Cell labeling

Cells were grown in ibidi™ petri dishes (ibidi, Martinsried, Germany) to confluency and treated with mild (200 mOsm), strong (80 mOsm) hypotonic and hypertonic (700 mOsm, 400 mM glucose) solutions for 0, 0.5, 2 and 6 h. Cells were fixed with 4% paraformadehyde PFA for 20 min. F-actin labeling was carried out with Alexa Fluor 546 phalloidin or 488 (Invitrogen, Darmstadt, Germany, diluted as recommended by the manufacturer, 5 μL methanolic stock solution with 200 μL PBS for each coverslip). For ezrin labeling, cells were incubated with primary monoclonal antibody (4 μg/mL diluted in PBS) for 1 h at room temperature and subsequently labeled with secondary Alexa Fluor 488-conjugated goat-anti-mouse IgG1 antibody (BD Biosciences, Heidelberg, Germany) for 45 min (4 μg/mL in PBS).

2.3. Atomic force microscopy for imaging

AFM imaging was performed with a Nanowizard® II AFM (JPK Instruments AG, Berlin) mounted on an Olympus IX 81 inverted light microscope. Although AFM delivers images of unprecedented resolution under physiological conditions, fixation of the plasma membrane for high resolution imaging is inevitable due to membrane flexibility and lateral mobility. Therefore, cells were fixated using 4% glutaraldehyde in PBS for 20 min. Silicon nitride cantilevers (MLCT, Bruker AFM Probes, Camarillo, USA) with a nominal spring constant of 0.01 N m^{-1} were employed. Cells were imaged in PBS at room temperature with a scan rate of 0.2 Hz and processed with JPK Image Processing® software.

2.4. Atomic force microscopy for elasticity measurements

Force curves were taken continuously on a Nanowizard™ II AFM (JPK Instruments AG, Berlin, Germany) while scanning laterally across the sample referred to as force mapping [11,12]. MDCK II cells seeded on Ibidi™ petri dishes (ibidi, Martinsried, Germany) and grown to confluency were mounted in a PetriDishHeater® (JPK Instruments AG, Berlin, Germany) set to 37 °C with HEPES buffered culture medium. Force curves were processed by applying an extended liquid droplet model first described by Sen et al. [13]. The contact angle of the spherical cap measured by AFM imaging for an untreated cell was found to be $\phi_0 = 20°$. For the radius of the cap we determined a value of 10 μm. Force curves are recorded in constant force (setpoint 1 nN). Further parameters are listed in Tables 1 and 2.

2.5. Atomic force microscopy for probing tether forces

Prior to tether pulling, cantilevers (MLCT, Bruker AFM Probes, Camerillo, USA) were plasma cleaned for 30 s (Argon) and incubated with 2.5 mg/mL concanavalin A (Sigma Aldrich, Germany) in PBS for 1.5 h to establish a strong contact to the apical surface. Both approach and retrace velocities were set to 2 μm/s. Tether forces were determined from force distance retrace curves (Fig. 4) and analyzed using Eq. (2).

3. Results

3.1. Mechanical theory—the liquid droplet model

The liquid droplet model successfully describes the viscoelastic behavior of neutrophils and leucocytes in micropipette aspiration experiments [14]. These cells behave like liquid drops when suspended and deform continuously inside a micropipette. Essentially, the model envisions the cellular interior as a homogeneous viscous liquid surrounded by a shell comprising the actomyosin cortex and the plasma membrane both exhibiting a static tension. Contributions from bending are neglected [15]. The model was successfully modified to describe the indentation of an AFM probe into an immobilized cell by Rosenbluth et al. [16] and Sen et al. for single adherent cells [13]. The model relies on the assumption that curvature and volume remain conserved throughout indentation. Two sources of restoring force occur, pre-stress or lateral tension in the membrane–cortex and the finite area compressibility upon in-plane stretching of the shell. The response to indentation originates almost exclusively from lateral stretching of the membrane and work against the existing pre-stress generated by the underlying cell cortex and the boundary, i.e. the cell–cell contacts. Here, we adopt this model to quantify the indentation of a conical indenter into a confluent cell represented by a spherical cap. The spherical cap represents the apical part of the cell in the context of a confluent cell layer. The model essentially assumes a lateral tension T composed of a lateral tension or pre-stress T_0 governing the response to indentation at low penetration depth and non-linear in-plane stretching of the shell characterized by a 2-D Hookean term [13]:

$$T = T_0 + \tilde{K}_A \frac{\Delta A}{A_0} \tag{1a}$$

Table 1
Parameters for modeling indentation of a spherical cap with a conical indenter describing confluent MDCK II cells subjected to hypotonic stress.

	Isotonic 300 mOsm	Hypotonic 200 mOm	Hypotonic 80 mOsm	Hypertonic 700 mOsm
ϕ_0 [°]	20	23	30	17
R_0 [μm]	35	30	26	28

Table 2
Parameters used for modeling MDCK II cells subjected to hypotonic stress (80 mOsm) over a time period of 6 h.

	1 h	2 h	3 h	4 h	5 h	6 h
ϕ_0 [°]	30	30	30	25	25	25
R_0 [μm]	26	26	26	38	38	38

with

$$\tilde{K}_A = K_A \frac{A_0}{A_0 + A_{ex}} \quad (1b)$$

ΔA denotes the change in surface area related to the initial area of the cell A_0. The apparent area compressibility modulus $\tilde{K}_A$ depends on the excess membrane area A_{ex} and the area compressibility modulus of the plasma membrane K_A usually around 0.1–0.4 N m^{-1}. Eq. (1b) implies that a large excess of surface area generates smaller apparent area compressibility modules. The lateral tension T_0 comprises the membrane's in-plane tension and contributions from adhesion of the cytoskeleton to the inner leaflet.

A second approach to measure the lateral tension of the plasma membrane comprises the extraction of membrane nanotubes also referred as membrane tethers from the apical plasma membrane. Tether formation is characterized by a force plateau followed by a sudden release of force due to tether rupture. This step is called the tether force F_{tether}. During tether formation additional membrane material from preexisting reservoirs is flowing into the growing tether. The force on the tether is directly connected to the in-plane tension T_{tether} and bending rigidity k of the membrane [17–20]:

$$F_{tether} = 2\pi\sqrt{2\kappa T_{tether}} \quad (2)$$

In indentation experiments cortical tension and membrane tension are not discernable, while tether pulling reports only on membrane tension. If both values match, neither cortical tension nor bending contributes to the elastic response of the cell. Therefore, if T_0 from indentation experiments matches the tension from tether pulling (Eq. (2)) it is safe to assume that the liquid droplet model applies to the cell type under investigation. While we found good accordance between the tension measured by indentation and tether pulling for MDCK II cells only poor correlation was observed for fibroblasts (data not shown).

3.2. Morphological changes of epithelial cell exposed to osmotic stress

The prerequisite of developing a comprehensive mechanical model that explains the interplay of membrane tension and surface area regulation was to examine the impact of osmotic stress on the morphology of the epithelial cell line MDCK II. Therefore, we challenged confluent cells for 30 min with solutions of different osmolarity and investigated the overall morphological response of the apical surface by recording images with an atomic force microscope. The topographical images provide information about roughness of the plasma membrane, height and diameter of the cell, and presence of protrusions such as microvilli. Under isoosmolar conditions we found well-established microvilli and the visible cell shape resembles a spherical cap with a height of 1 μm and radius of 10 μm (median), respectively (Fig. 1A, E, I, and J). Under mild hypotonic stress (200 mOsm) the cell size increases but the plasma membrane surface still displays microvillar structure (Fig. 1B and F) from which we conclude that the membrane is still attached to the cortex. While the radius of the cells is conserved, the height of the spherical cap increases from 1 to 1.7 μm (median) demonstrating a swelling of the cell. The most prominent change in surface structure and cell height is visible for cells challenged with a strong hypotonic solution (80 mOsm) (Fig. 1C). Microvilli are largely removed generating a smooth membrane surface (Fig. 1C and G). The height of the highly stressed cells increases up to 2.8 μm (height of the spherical cap) (Fig. 1I). We also investigated the impact of hypertonic stress on cellular morphology. Although the topographical image shows no significant impact of the treatment (Fig. 1H), we observe changes in cell height and cell radius (Fig. 1D). While hypoosmotic stress leads to cell swelling, the inverse treatment leads to shrinkage of cells to a height of merely 0.6 μm and a radius of 7 μm (median) (Fig. 1I and J). Analyzing the cellular shape and surface structure after application of osmotic stress enables us to collect important geometrical input parameters for our mechanical model (vide infra) (Fig. 1K).

A spherical cap essentially captures the general shape of the apical part of cells in a confluent monolayer in the most simplistic way. The cap is characterized by a contact angle and radius at the base (or alternatively the height of the cap), which are crucial and sufficient to describe the shape of the cell upon indentation according to the liquid droplet theory of Sen et al. [13] (vide supra).

3.3. Mechanical response to hypoosmotic stress

Cells swell under hypoosmotic conditions and thereby deform and generate hydrostatic pressure against the plasma membrane. We investigated this effect by indentation as well tether pulling experiments using force microscopy carried out with an AFM. Indentation experiments yielding force distance curves (Fig. 2A) provide access to mechanical parameters like the apparent area compressibility modulus $\tilde{K}_A$, which reflects changes in effective membrane area (Eq. (1b)), and the lateral membrane tension (pre-stress) T_0. The area compressibility modulus relates to κ, the bending modulus ($K_A \propto \kappa d^{-2}$) of the membrane–cortex composite and E_Y, the Young's modulus $K_A \propto E_Y\ d$ of the cortex (d denotes the thickness of the shell). Force distance curves taken on osmotically stressed cells display a substantial change in the slope (Fig. 2A). While a mild hypoosmotic solution (200 mOsm) shows almost no change in the shape of the approach curve, a lowering of the external osmolarity to 80 mOsm leads to a larger indentation depth at constant force, clearly indicative of a softening of the cells assembly mirrored in reduced values for T_0 and $\tilde{K}_A$. In fact, exposing cells to a strong hypotonic solution (80 mOsm) results in the same degree of cell softening as obtained from experiments where the F-actin cytoskeleton is destroyed by administration of cytochalasin D. This suggests that during hypoosmotic stress the deformation and outward bulging of the plasma membrane induced by the large internal pressure could lead to a reorganization of destruction of the cytoskeleton in response to the external force [21]. In consequence, the cytoskeletal contribution to membrane tension is diminished.

The mechanical parameters obtained from the indentation experiments under mild hypoosmotic stress display, however, a significant increase in tension T_0 ((0.35 ± 0.1) mN m^{-1}, median; isotonic (0.29 ± 0.09) mN m^{-1}, median) and area compressibility modulus $\tilde{K}_A$ ((0.06 ± 0.09) N m^{-1}, median; isotonic (0.03 ± 0.08) N m^{-1}) compared to isotonic conditions. The reduction in excess membrane area, mirrored in an increase of $\tilde{K}_A$ (according Eq. (1b)), is attributed to cell swelling smoothing out membrane reservoir [10]. Cell swelling exerts a pressure differences across the plasma membrane and inevitably increases the membrane's in-plane tension according to Laplace's law. A rise in tension implies that the cell is not able to quickly respond by providing excess area stored in protrusions and invaginations of the plasma membrane to counterbalance the rising tension since the increased cell volume diminishes this excess membrane.

In order to obtain a more comprehensive picture of the destructive nature of strong hypoosmotic stress we also investigated the structural changes of the F-actin cytoskeleton by fluorescence staining. Fig. 3 shows how the F-actin rearranges as a function of osmolarity.

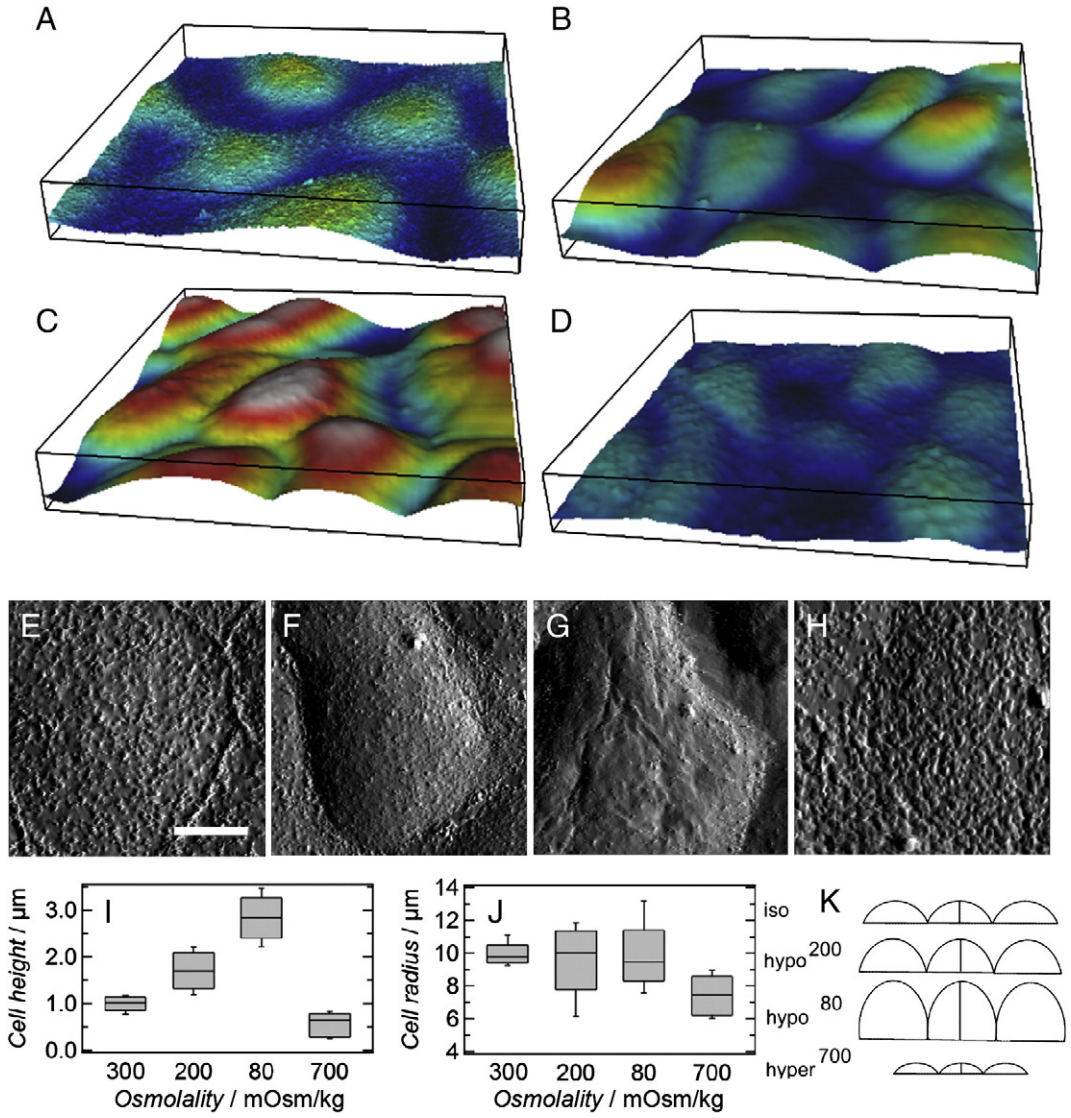

Fig. 1. Morphological changes of confluent MDCK II cells after exposure to osmotic stress. (A–D) 3D-height images of confluent MDCK II cells treated with different osmotic solutions. (A) Isotonic. (B) 200 mOsm. (C) 80 mOsm. (D) 700 mOsm. Height of the box is 5 µm, box length and width are 50 µm. (E–H) AFM deflection images to visualize membrane protrusions, scale bar is 10 µm. (E) Untreated cell (300 mOsm). (F) 200 mOsm. (G) 80 mOsm. (H) 700 mOsm. (I) Cell height. (J) Cell radius, extracted from AFM height images, at least $n = 10$ cells. (K) Schematic drawing of spherical caps that emerge from the cell monolayer beyond the cell–cell contacts to illustrate change in cell size as a result of osmotic treatment.

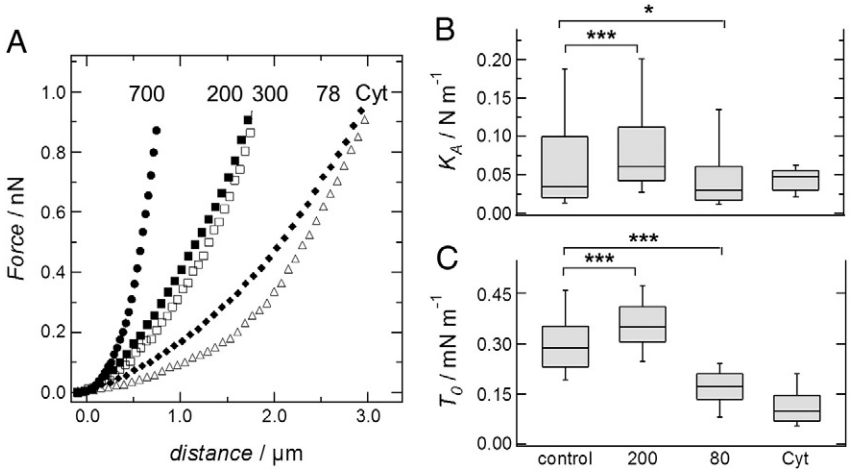

Fig. 2. Indentation experiments revealing mechanical information of hypoosmotically stressed confluent MDCK II cells. (A) Representative force distance traces taken on treated cells. Trace curve is fitted with a modified liquid droplet model for indentation experiments to provide estimates of the apparent area compressibility module $\tilde{K}_A$ and tension (pre-stress) T_0. (B) Apparent area compressibility modulus $\tilde{K}_A$, reflecting the changes in membrane area as a function of osmolarity. (C) Changes in membrane tension T_0 by altering the osmotic stress or F-actin integrity by cytochalasin D (⁎ corresponds to $p<10^{-2}$; ⁎⁎⁎ to $p<10^{-3}$, two-tailed Wilcoxon rank sum test).

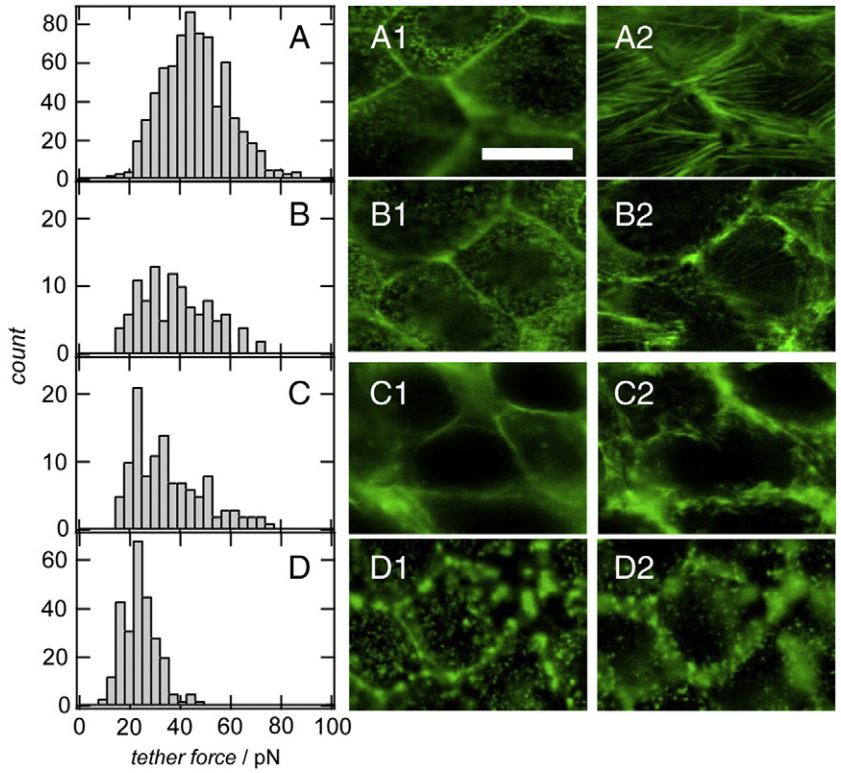

Fig. 3. Histogram of tether forces obtained from retrace curves of a force cycle recorded on MDCK II cells exposed to different osmotic stress with corresponding fluorescence micrographs of MDCK II cells. (A) Histogram of tether forces of untreated cells (isotonic, 300 mOsm). A1 shows apical part of the cell, A2 the corresponding basolateral part. (B) 200 mOsm. (C) 80 mOsm. (D) Cells treated with cytochalasin D destabilizing F-actin. Scale bar is 20 μm.

The fluorescence micrographs display no change in the structure of the cortical F-actin at the apical part of the cells after treatment with mild hypotonic solution (Fig. 3B1). In the basolateral region, however, an alteration in the formation of stress fibers is observed (Fig. 3B2). Comparing with an untreated sample, the structure of the stress fibers is less pronounced.

Indentation experiments are supported by tether pulling experiments taken on the same spot. Tether formation provides and independent means to access membrane's in-plane tension without interference from cell shape changes and mechanical response to the cytoskeleton except for its adhesive properties. Therefore, we functionalized AFM tips with concanavalin A providing enough non-specific adhesion to extract membrane nanotubes from the apical membrane. From the force plateau (F_{tether}) of a fully established membrane nanotube, we calculate the membrane tension T_{tether} according to [20,22] (Fig. 4A).

Membrane tension contains contribution from membrane–cytoskeleton adhesion as well as tension in the bilayer itself [22]. In general, tension values obtained from tether pulling are very similar to those assessed by indentation experiments largely confirming the assumed liquid droplet model to describe indentation experiments. Interestingly, however, mild hypotonic conditions produce a decrease in membrane tension T_{tether} determined from tether pulling in contrast to the tension T_0 obtained from indentation experiments (T_{tether} (200 mOsm) $= 0.17 \pm 0.11$ mN m^{-1}, median; T_{tether} (isotonic) $= 0.25 \pm 0.13$ mN m^{-1}, median). A possible explanation is the outward directed osmotic pressure that would facilitate tether pulling but aggravate indentation. Increasing the swelling process by using a strong hypoosmotic solution leads to a change in the apparent area compressibility modulus, in particular the loss of the higher values, which are attributed to regions on the cell surface with direct connection to the underlying cytoskeleton (Fig. 2B). At the same time, membrane tension T_0 decreases to a value of 0.17 ± 0.05 mN m^{-1} (median) (Fig. 2C). Although the cells increase their volume by swelling this leads to a softening of the cells mainly due to removal of adhesion between the cortex and the inner leaflet. The F-actin cytoskeleton shows a dramatic reorganization by strong osmotic challenge (80 mOsm). In the apical region, no microvilli or cortical

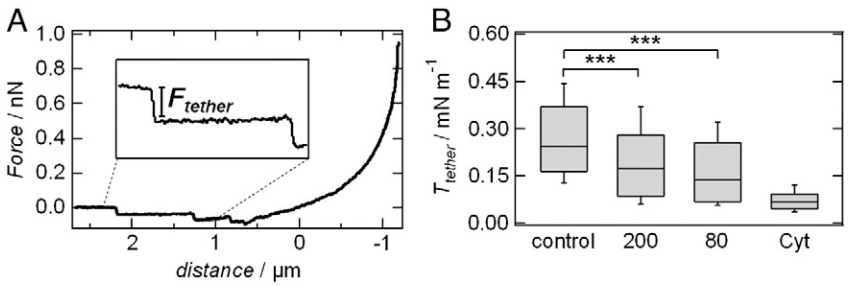

Fig. 4. (A) Retrace curve displays tether formation obtained from a force cycle. (B) Membrane tension T_{tether} calculated from tether pulling experiments (Eq. (2)). For computing T_{tether} we chose a bending module κ of 10^{-19} J representing fluid lipid bilayer. Viscous contributions to the tether force (~7 pN) are neglected as a first approximation [39,40].

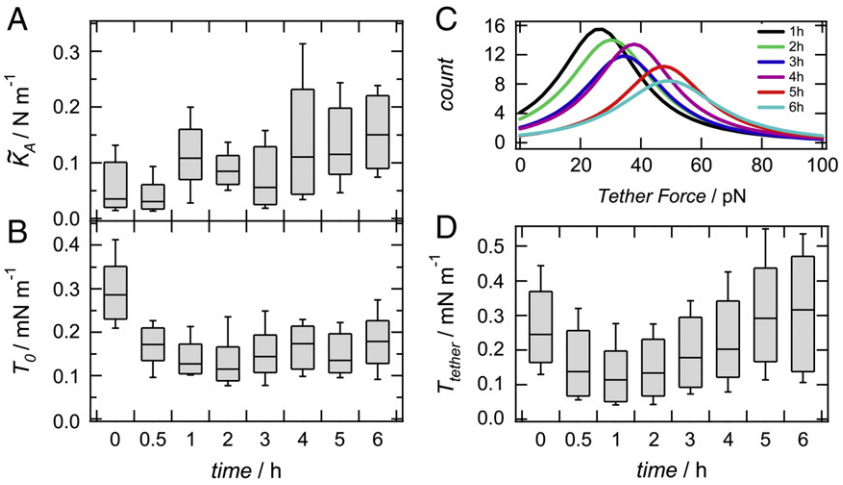

Fig. 5. Mechanical changes resulting from prolonged incubation in hypoosmotic solution. (A) Apparent area compressibility modulus measured at different time points. (B) Membrane tension obtained from indentation experiments. (C) Lorenz–Fits of tether force histograms as a function of time. (D) Membrane tension T_{tether} calculated from tether pulling experiments (Eq. (2)).

structures are visible in the fluorescence micrographs. Stress fibers are completely degraded (Fig. 3). Concomitantly tether forces are shifted to lower values (Fig. 3), resulting from a decreased membrane tension (0.14 ± 0.12 mN m^{-1}, Fig. 4B). A similar disassembly of the cortical cytoskeleton and stress fibers can be achieved by treating the cell with cytochalasin D. From the fluorescence micrograph shown in Fig. 3D1 and D2 the reorganization of the actin cytoskeleton after administration of cytochalasin D is visible. In the apical part of the cell the cortical actin is severed and condensed into small cluster. Additionally, the basal region is devoid of stress fibers [23]. This leads to a decreased membrane tension, measured by indentation and tether pulling (Fig. 2C, 3, and 4).

We found that destruction of the F-actin cytoskeleton with a drug such as cytochalasin D displays a similar change of the relevant mechanical parameters such as tension and area compressibility as hypoosmotic stress, although the cells are increasing their volume due to swelling. This leads us to the assumption that the cell responds to membrane deformation and increased membrane tension induced by osmotic swelling due to hypoosmotic stress by disassembly of the cytoskeleton to release tension. The accompanying release of tension prevents plasma membrane lysis, which would inevitably destroy the cell.

3.4. Cells regulate membrane tension/area during prolonged hypoosmotic challenge

So far, we could show that plasma membrane tension drops in response to strong hypoosmotic stress and propose that the accompanying deformation of the membrane, a result from cell swelling, remodels up the F-actin cytoskeleton to release tension that prevents lysis of the membrane [2]. The question arises, how the cells will respond to the altered environmental conditions on longer time scales. Will the cell faster endocytosis to compensate for the drop in membrane tension to restore its initial value? No active surface regulation was observed in the above-described experiments lasting only 30 min. Therefore, we extended the observation period considerably allowing us to investigate the mechanical properties of a confluent MDCK II monolayer during strong hypoosmotic stress over more than 6 h (Fig. 5). Mechanical experiments were continuously carried out to document the changes in tension and surface area during this time period. The apparent area compressibility modulus $\tilde{K}_A$, reflecting the change in membrane area, increases continuously within this observation time from 0.03 ± 0.08 N m^{-1} (median) up to 0.15 ± 0.07 N m^{-1} (median) (Fig. 5A) indicative of loss of membrane material.

For untreated cells the $\tilde{K}_A$ value reflects a membrane folding factor of 6 assuming an area compressibility modulus of 0.17 N m^{-1} for the plasma membrane. Such a value is typical for lipid bilayers emphasizing the inextensibility of the membrane [24]. Therefore, we can conclude that virtually no excess area remains after 6 h of exposure to hypoosmotic stress. During initial swelling the apparent area compressibility modulus is not affected (0.5 h $\tilde{K}_A$, 0.03 ± 0.06 N m^{-1} (median)), while membrane tension (T_0 and T_{tether}) decreases, indicating a change in the cytoskeleton architecture. After 1 h of incubation time, the cells start to regulate the membrane area, i.e. remove excess area (Fig. 5A) (Table 3). We found a higher endocytosis rate as a response to 2 h of strong hypoosmotic stress (Fig. 6), i.e. a larger number of vesicles accumulating in the cytosol. At this time point, recovery of membrane tension estimated from tether pulling experiments has completed (Fig. 5D) (Table 3). As shown in Fig. 5C, during 6 h of incubation, tether forces shifted to higher values comparable to values obtained from untreated cells (Fig. 3A). It should be noted that both values $\tilde{K}_A$ and T_{tether} increase indicating a plasma membrane regulatory effect. While the tension T_{tether} from tether pulling experiments largely recovers to its initial values, tension obtained from indentation experiments T_0 show only a moderate recovery to values of about 0.18 ± 0.06 mN m^{-1}. Notably, the tether force mainly comprises contributions from membrane adhesion to the cytoskeleton, while the value of T_0 might also include other elastic contributions from the membrane–cortex composite and is more strongly affected by the cell's shape. Tension can generally be actively increased by establishing a

Table 3
Mechanical parameters obtained from prolonged incubation in hypoosmotic solution. Values represent the median obtained from box plots in Fig. 6 and the median's absolute deviation.

Incubation time [h]	0	0.5	1	2	3	4	5	6
K_A [N m^{-1}]	0.03 ± 0.08	0.03 ± 0.06	0.11 ± 0.06	0.08 ± 0.02	0.06 ± 0.06	0.11 ± 0.11	0.12 ± 0.07	0.15 ± 0.07
T_0 [mN m^{-1}]	0.29 ± 0.09	0.17 ± 0.06	0.13 ± 0.04	0.12 ± 0.06	0.14 ± 0.06	0.17 ± 0.05	0.14 ± 0.06	0.18 ± 0.06
T_{tether} [mN m^{-1}]	0.25 ± 0.13	0.14 ± 0.12	0.11 ± 0.1	0.13 ± 0.09	0.18 ± 0.09	0.2 ± 0.13	0.29 ± 0.13	0.32 ± 0.15

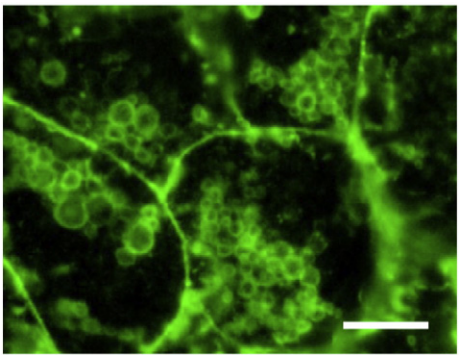

Fig. 6. Micrograph of confluent MDCK II cells challenged with a strong hypoosmotic solution (80 mOsm) for 2 h. F-actin is labeled in green (Alexa Fluor 488). Scale bar 10 μm.

larger number of molecular-anchors to the underlying cortex. To examine whether this takes place, we fluorescently labeled ezrin, a member of the ERM family that is known to connect F-actin to the apical plasma membrane. Structural organization and stabilization of the plasma membrane protrusions relies heavily on protein linkers such as ezrin connecting the cellular membrane via PIP_2 to microfilaments [25,26].

We observe a change in the ezrin and F-actin distribution during prolonged exposure to hypoosmotic stress (Fig. 7). After 2 h of incubation the density and distribution of the protein ezrin is decreased in the apical region (Fig. 7B1). Concomitantly, the cortical F-actin structure is altered. In the lower part of the cell, in which the isotonic sample exhibits stress fibers (Fig. 7A4), the hypoosmotically stressed cell displays a disassembled F-actin structure. This situation remains unchanged during the following 6 h of observation time (Fig. 7C4), where the basal F-actin structure is indistinguishable from the one after 2 h. However, the apical structure (ezrin and F-actin distribution) shows a similar composition as the isotonic control cells after 6 h. This is in good accordance with our mechanical experiments that also show a recovery of tension with time. After 6 h the tension is largely restored and the same number of ezrin mediated F-actin-membrane contacts reached. Taken together, the apical membrane–cortex structure reforms under stress, while the basolateral side does not recover.

This finding provides a possible explanation the different values of membrane tension obtained from indentation (T_0) and tether pulling (T_{tether}). While tension estimated from tethers (T_{tether}) draws its value mainly from membrane–cytoskeleton adhesion and therefore increases over time, tension obtained from indentation (T_0) also comprises elastic contributions from the whole cell and requires an intact cortex shell, which is still not fully restored after 6 h exposure to hypoosmotic stress.

In summary, strong hypoosmotic stress lasting for 30 min leads to a swelling of the MDCK II cells accompanied by a decrease in membrane tension (T_0 and T_{tether}) and a dramatic alteration of the F-actin structure. Longer treatment of MDCK II cells (6 h) shows a stepwise increase in the apparent area compressibility modulus and larger amount of membrane–actin contacts to restore membrane tension prior to the stimulus.

3.5. Hyperosmotic shock: From liquid droplet to a drum like geometry

So far, we dealt with the mechanical response of cells within a confluent monolayer to exposure to hypotononic solutions. But what happens, if the cell experiences hypertonic stress? Will the excess supply of membrane area lead to a sudden drop in tension? We described the morphological changes during a hypertonic shock in Fig. 1. In essence, we found that the cells shrink in height and diameter. This extreme shape change towards a more two dimensional drum-like apical side has an important impact on the determination

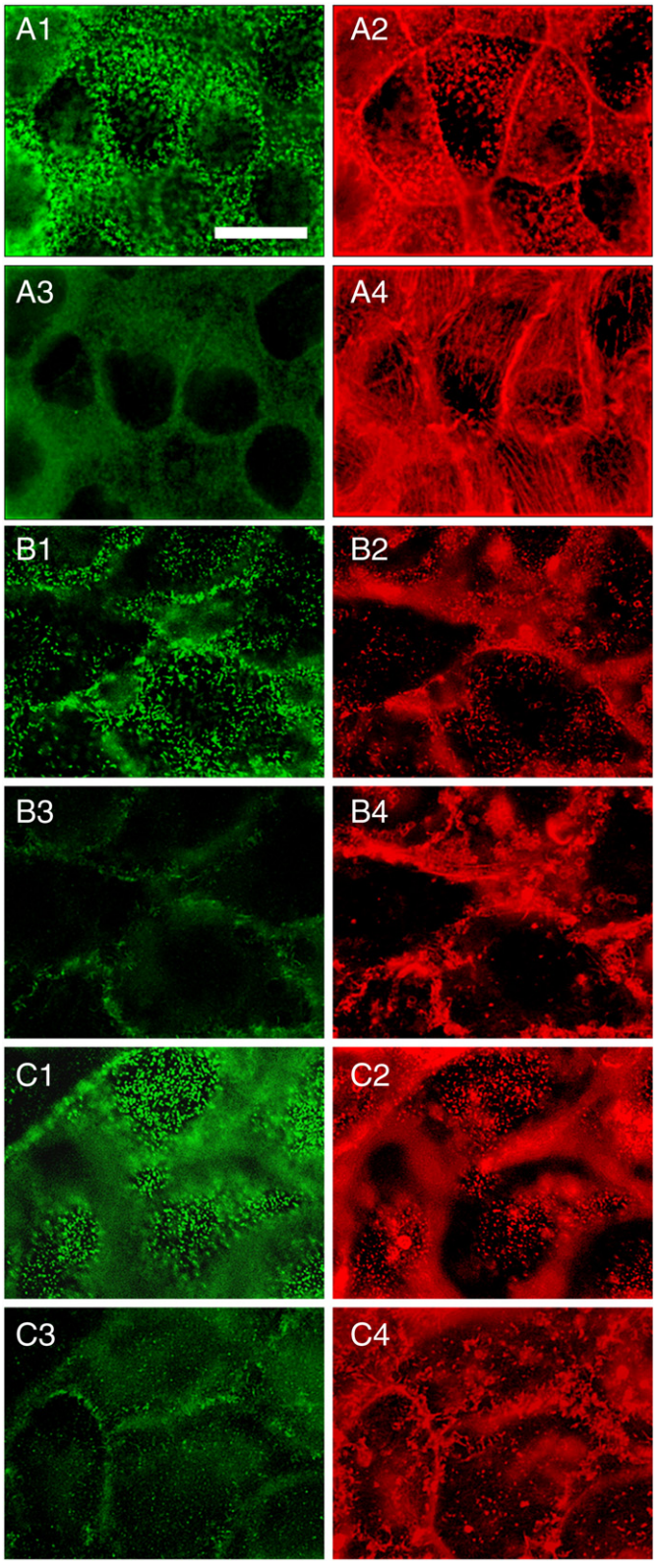

Fig. 7. Fluorescence micrographs of confluent MDCK II cells exposed for 0 h (A), 2 h (B) and 6 h (C) to strong hypoosmotic solution (80 mOsm). Microfilament–membrane anchor protein ezrin is labeled in green (Alexa Fluor 488), F-actin in red (Alexa Fluor 546). Scale bar is 20 μm.

of mechanical parameters obtained from indentation as well as tether pulling experiments. In Fig. 2 we display force distance traces taken on osmotically challenged cells. Cells stressed with hyperosmotic solution show the steepest slope indicating a rigid or even solid-like

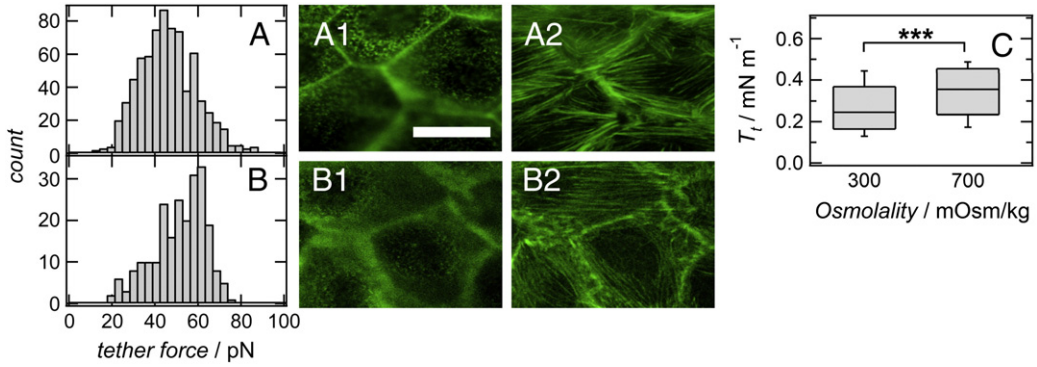

Fig. 8. (A) Histograms of tether forces obtained from experiments of hypertonically (700 mOsm) challenged cells compared to a control (308 mOsm). Fluorescence micrographs of F-actin labeled MDCK II cells treated with isotonic (A1: apical, A2: basal) and hypertonic (B1: apical, B2: basal) solution for 30 min. Scale bar is 20 μm. (C) Membrane tension, T_{tether}, estimated from tether pulling experiments according to Eq. (2).

appearance. Concomitantly, tether forces are shifted to higher values compared to control cells (Fig. 8B). Estimating membrane tension according Eq. (2) from tether forces we found an increase from 0.25 ± 0.13 mN m^{-1} (median, isotonic) to 0.36 ± 0.13 mN m^{-1} (median, hypertonic) (Fig. 8C). Because of the extreme shrinkage of the cell by a factor of almost 2 (Fig. 1), the cells can no longer be regarded as a liquid droplet in spherical cap geometry. Assuming a drum-like architecture, which is essentially described by a 2-D planar circular membrane indented in the center by a point load force, we can apply the following Eq. (3) derived by Komaragir et al. [27,28] to analyze the force-indentation curves.

$$F(h) = \pi T_0 h + \frac{\pi K_A}{3R^2} h^3 \tag{3}$$

The first term is linear in penetration depth h and dominated by pre-stress (tension) T_0 in the membrane. The second term captures lateral stretching of the membrane and solely depends on the membrane's area compressibility modulus K_A. The radius of the circular membrane framed by the tight junctions of the adjacent cells is denoted by R.

The values for $\tilde{K}_A$ obtained from fitting the parameters of Eq. (2) to the force indentation curves increase upon exposure to hyperosmotic stress indicative of reduction of surface area, while T_0 decreases (Table 4).

Importantly, this implies that the substantial changes in the force indentation curve are mainly due to changes in cell morphology, i.e. geometry and not so much due to changes in elastic properties. This finding is corroborated by tether pulling experiments. In tether pulling experiments, the distribution of tension values only slightly shifts to higher values upon exposure to hypertonic solutions. The following scenario is conceivable. Tension of the bilayer drops due to osmotic pressure changes and the membrane collapses on the cytoskeleton. In turn, excess membrane area is removed by endocytosis and tension largely restored since the remaining osmotic pressure forces the membrane onto the cortex producing larger tether forces due to the additional pressure difference.

Table 4
Mechanical parameters obtained from hypertonic stress on confluent MDCK II cells.

	K_A Eq. (2) [N m^{-1}]	Radius [μm]	T_0 Eq. (2) [mN m^{-1}]	T_{tether} [mN m^{-1}]
Hypertonic	0.29 ± 0.21	7.7 ± 1.35	0.11 ± 0.09	0.35 ± 0.17

3.6. Cellular response to distilled water

The strongest hypotonic stress is exerted to the cells by exposing them to distilled water (1 mOsm). This treatment leads to an extreme volume increase and eventually to cell lysis (Fig. 9B, white arrow) upon exposure to distilled water for longer than 30 min or application of external force exerted by an indenter (AFM tip).

This osmotically enforced membrane area increase cannot be balanced by surface area regulation. Inevitably, this treatment leads to membrane lysis. Force distance curves recorded on these tremendously swollen cells display a substantially steeper slope compared to untreated cells (Fig. 9C). The cytosolic pressure acting on the membrane results in a very high tension inside the bilayer, which cannot be buffered by reservoirs since they are exhausted due to the sudden volume increase. In order to place these experiments in a mechanical context, a Hertzian contact model is used [29–33]. The Young-modulus of MDCK II cells exposed to distilled water yield elevated values of $E = 30$ kPa ± 17 kPa. This is an increase in cell elasticity by a factor of 5 compared to untreated cells [21,30]. The attempt to pull out membrane nanotubes of the plasma membrane of MDCK II cells exposed to distilled water fails since reservoirs are exhausted.

4. Discussion

Here, we investigated the impact of osmotic stress on the mechanical properties of the kidney epithelial cell line MDCK II with the AFM in a spatial–temporal fashion. Confluent monolayers were chosen to mimic tissue behavior in contrast to single isolated cells. We first examined the morphological changes due to hypoosmotic stress by analyzing AFM height images. We observed an increase in cell height, while the diameter of the apical caps was preserved. The cell surface is increased at mild hypotonic treatment by a factor of 1.7 and at strong hypotonic stress by a factor of 2.7. This is in accordance with observations from Groulx and coworkers who found a 3.6-fold increase in surface area for mammalian cells 98% hypoosmotic solution [8]. As the plasma membrane is largely inextensible and cannot bear large strains due to its liquid-crystalline nature, limiting critical area dilatation to 3–4% [9], changes in surface area require a rapid response to maintain constant membrane tension in order avoid lysis. Cells increase their surface to avoid lysis due to volume increase by drawing additional membrane from preexisting reservoirs [10], which is visible in the AFM-topographical images. Upon exposure to strong hypotonic solution the cell surface is smoothened out since membrane protrusions like microvilli disappear during cell swelling. Sukhorukov et al. could show by impedance measurements that hypo-osmotically stressed cells obtain the necessary membrane area by using material from microvilli [34]. This membrane deformation has a detectable impact on the cellular mechanics. By performing

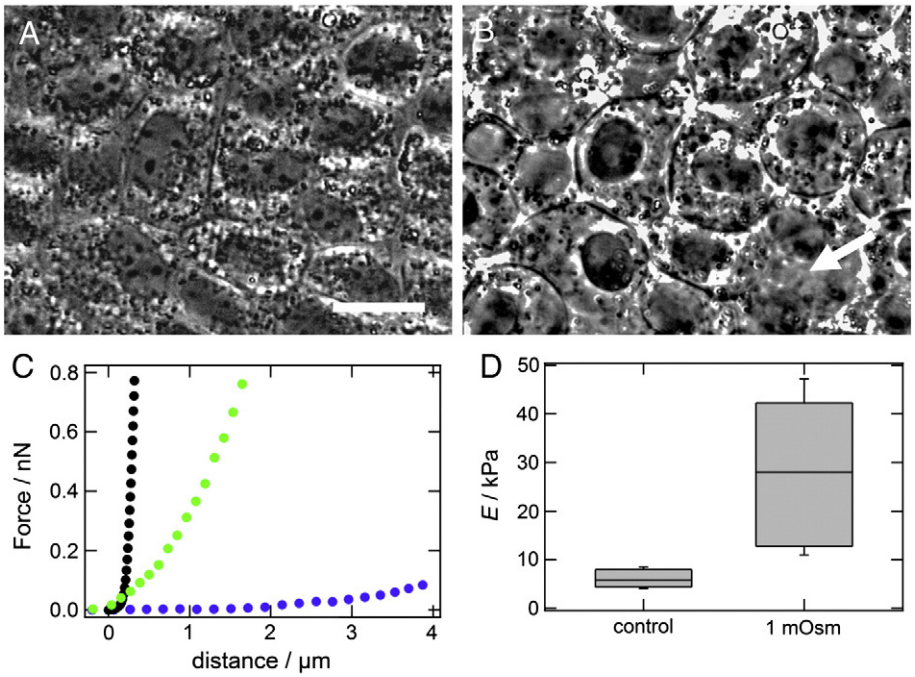

Fig. 9. Phase contrast micrographs of MDCK II cells before (A) and after exposure to distilled water (B). The white arrow in right corner of image B indicates a ruptured cell. Scale bar 20 µm. (C) Force indentation curves recorded on MDCK II cells after different treatments. (●) Green dots display mechanical response of untreated cells to indentation. (●) Black dots cells during exposure to distilled water. (●) blue dots mark cells exposed to distilled water after repetitive indentation. Occasionally cell lysis of the stressed cells occurs. (D) Young-modulus of cells treated with very low osmolarity (distilled water) ($n = 5$ cells).

indentation and tether pulling experiments we were able to show how cells respond to swelling or shrinking to maintain cell integrity and avoid lysis. A mild hypotonic stress leads to an increase in membrane tension because of the additional pressure difference acting against the membrane. The apparent area compressibility modulus also increases upon exposure to hypotonic solution reflecting a 2-fold loss of excess membrane. This mild effect changes if the cells are subjected to stronger hypotonic stress. We observe a reorganization of the F-actin cytoskeleton, allowing the tension to relax. The phenotype resembles cells treated with cytochalasin D also producing the same mechanical properties. Guilak and coworkers could also detect a decrease in the elastic module and F-actin distribution of chondrocytes by hypoosmotic challenge [21,35,36]. The remodeling of the cytoskeleton leads to a tension decrease and concomitantly to additional membrane area released from bound membrane reservoirs such as microvilli. This scenario is confirmed by the fact that the apparent area compressibility modulus decreases considerably in response to strong hypotonic treatment. We interpret this sudden release of membrane material as a first line response to protect the cells from lysis due to swelling (Fig. 10). The restoration of cell size under continuous hypotonic stress is known as regulatory volume decrease (RVD) [37]. During the experimental duration (30 min) we detect no such regulatory effect. As a consequence, the cell requires a fast response system to cope with mild to moderate changes in osmotic pressure. The question was now, whether the cells adapt to the situation by restoring some of the lost contacts between the membrane and the cytoskeleton and as a consequence regain the original membrane tension prior to exposure to hypoosmotic solutions. Therefore, we extended the exposure time to hypotonic solutions to more than 6 h and found that the cell indeed largely restores its initial tension prior to exposure to hypertonic solutions. The accompanying increase in the apparent area compressibility modulus reflects how the cells accomplishes this task, namely by a reduction in surface area that is necessary to restore the tension. This picture is confirmed by fluorescence micrographs displaying enhanced endocytosis. The apparent area compressibility modules measured 6 h after exposure to hypotonic solutions are virtually identical to those that measured for neat lipid bilayer lacking membrane reservoirs. A stronger adhesion to the cortex can be clearly inferred from tether pulling experiments producing stronger tether forces with time, while fluorescence microscopy shows an increasing amount of ezrin and actin at the apical side. This means that the cells have sacrificed a large portion of the excess surface stored in protrusions and invaginations to restore the original tension. Probably this is at the upper limit for osmotic stress cell can bear without damage. Interestingly, the basal side of the polar epithelia seems to be less prone to remodeling of the actin cytoskeleton (lack of stress fibers), which suggests that the process of adaption has not been finished yet.

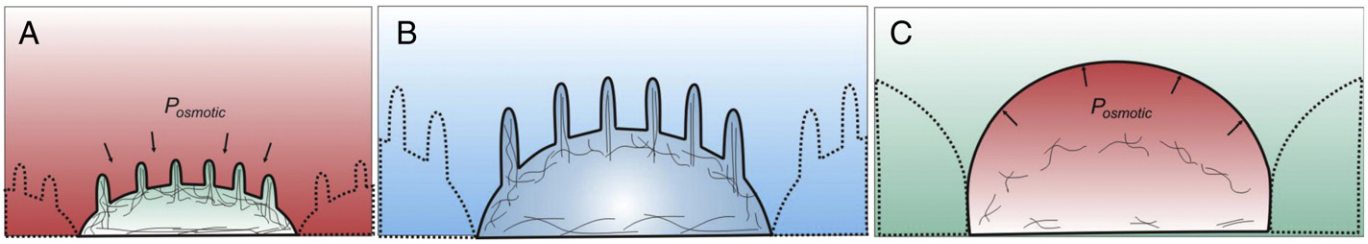

Fig. 10. Schematic illustration of osmotic challenged MDCK II cells. (A) Cell shrinkage due to hyperosmotic stress acting outwards on the plasma membrane. (B) Cells under isotonic conditions exhibiting membrane reservoirs and an intact underlying cortex. (C) Cell swelling due to osmotic pressure acting against the internal plasma membrane (hypoosmotic conditions) rupturing the cortex.

In contrast to hypotonic stress, hyperosmolar stress merely leads to collapsing of the membrane onto the actin cortex (Fig. 10). As a consequence, the cell morphology changes tremendously, which impacts the appearance of force indentation curves severely. The cells appear now much stiffer, which is mainly a product of the switch in topography rather than a sudden increase in stiffness. By accounting for the changed geometry we arrive at reasonable values for the area compressibility modulus and tension that deviate only slightly from those of untreated cells. Tension values derived from tether experiments are less compromised by other elastic contributions and report that tension slightly increases. Tension derived from indentation might also comprise elastic contributions from bending.

Exposing confluent MDCK II cells to very low osmolarity (1 mOsm, distilled water) generates a tremendous volume change [8,38]. The high cytosolic pressure of the cytosol bends the plasma membrane and produces considerable tension inside the bilayer according to Laplace's law that might be close to lysis tension [10]. Consequently, also tether pulling experiments fail, since the formation of tethers require the existence of membrane reservoirs that have been exhausted during swelling. Additional external stress exerted on osmotically swollen MDCK II cells by indentation frequently leads to lysis. In conclusion, the experiments can be cast into a conclusive model that explains qualitatively as well as quantitatively the response of confluent epithelial cells to osmotic stress by sacrificing existing membrane reservoirs.

5. Conclusions

In summary, we could show that cells in the context of confluent monolayers adapt to hypoosmotic challenges in two ways. One quick, purely physical response is found relying entirely on the available membrane surface reservoirs and dissolution of the cytoskeleton preventing lysis of the plasma membrane and a second long-term response involving remodeling of the cytoskeleton-membrane junction and increased endocytosis to regain the initial tension by reestablishing connections to the plasma membrane. The scenario of hypoosmotic challenges can therefore be envisioned as follows: under isotonic conditions the (isotropic) tension of the plasma membrane is produced by molecular contacts between the actin cytoskeleton and the membrane. The apparent area compressibility modulus, which describes the membrane's resistance to in-plane stretching, mirrors excess area stored in protrusions and invaginations. Mild hypotonic conditions do not visibly affect the integrity of the cortex and, as consequence, do not disconnect the membrane from the cytoskeleton. As a consequence, the apparent area compressibility modulus increases to respond to the increase in tension due to swelling. The resulting change in volume compensates for the increased osmotic pressure. Tether pulling experiments reveal a drop in tension that we attribute predominately to a loss in actin-membrane contacts. Indentation experiments, however, show an increase in tension that is probably due to the additional osmotic pressure resisting indentation. The opposite is found for application of hypertonic stress. Tether forces increase due to inward osmotic pressure, while the tension inferred from indentation experiments is lower.

Strong hypoosmotic stress eventually leads to disintegration of the cortex and lift-off of the plasma membrane. Concomitantly, the apparent area compressibility modulus decreases indicative of allocation of excess membrane area. The loss of membrane–actin contact leads to strong swelling of the cell body and, as a consequence, tension drops since the cortex no longer supports the plasma membrane. However, the process is reversible and over time cortical tension is reestablished while excess membrane area is consumed by increased endocytosis.

Acknowledgments

Financial support by the DFG (SFB 937) is gratefully acknowledged. A.P. is financially supported by the Dorothea Schlözer Foundation of Georg-August-University.

References

[1] J. Dai, H.P. Ting-Beall, M.P. Sheetz, The secretion-coupled endocytosis correlates with membrane tension changes in RBL 2H3 cells, J. Gen. Physiol. 110 (1997) 1–10.
[2] G. Apodaca, Modulation of membrane traffic by mechanical stimuli, Am. J. Physiol. Renal Physiol. 282 (2002) 179–190.
[3] M.P. Sheetz, J. Dai, Modulation of membrane dynamics and cell motility by membrane tension, Trends Cell Biol. 6 (1996) 85–89.
[4] N.C. Gauthier, M.A. Fardin, P. Roca-Cusachs, M.P. Sheetz, Temporary increase in plasma membrane tension coordinates the activation of exocytosis and contraction during cell spreading, Proc. Natl. Acad. Sci. 108 (2011) 14467–14472.
[5] D. Raucher, M.P. Sheetz, Cell spreading and lamellipodial extension rate is regulated by membrane tension, J. Cell Biol. 148 (2000) 127–136.
[6] D. Raucher, M.P. Sheetz, Membrane expansion increases endocytosis rate during mitosis, J. Cell Biol. 144 (1999) 497–506.
[7] J. Dai, M.P. Sheetz, Membrane tether formation from blebbing cells, Biophys. J. 77 (1999) 3363–3370.
[8] N. Groulx, F. Boudreault, S. Orlov, R. Grygorczyk, Membrane reserves and hypotonic cell swelling, J. Membr. Biol. 214 (2006) 43–56.
[9] C.E. Morris, U. Homann, Cell surface area regulation and membrane tension, J. Membr. Biol. 179 (2001) 79–102.
[10] L. Kozera, E. White, S. Calaghan, Caveolae act as membrane reserves which limit mechanosensitive I(Cl, swell) channel activation during swelling in the rat ventricular myocyte, PLoS One 4 (2009) e8312.
[11] M. Radmacher, M. Fritz, C.M. Kacher, J.P. Cleveland, P.K. Hansma, Measuring the viscoelastic properties of human platelets with the atomic force microscope, Biophys. J. 70 (1996) 556–567.
[12] H. Haga, S. Sasaki, K. Kawabata, E. Ito, T. Ushiki, T. Sambongi, Elasticity mapping of living fibroblasts by AFM and immunofluorescence observation of the cytoskeleton, Ultramicroscopy 82 (2000) 253–258.
[13] S. Sen, S. Subramanian, D.E. Discher, Indentation and adhesive probing of a cell membrane with AFM: theoretical model and experiments, Biophys. J. 89 (2005) 3203–3213.
[14] A. Yeung, E. Evans, Cortical shell-liquid core model for passive flow of liquid-like spherical cells into micropipets, Biophys. J. 56 (1989) 139–149.
[15] C.T. Lim, E.H. Zhou, S.T. Quek, Mechanical models for living cells–a review, J. Biomech. 39 (2006) 195–216.
[16] M.J. Rosenbluth, W.A. Lam, D.A. Fletcher, Force microscopy of nonadherent cells: a comparison of leukemia cell deformability, Biophys. J. 90 (2006) 2994–3003.
[17] R.E. Waugh, R.M. Hochmuth, Mechanical equilibrium of thick, hollow, liquid membrane cylinders, Biophys. J. 52 (1987) 391–400.
[18] E.A. Evans, R. Skalak, Mechanics and thermodynamic of biomembranes: Pt. 1, 1979.
[19] F.M. Hochmuth, J.Y. Shao, J. Dai, M.P. Sheetz, Deformation and flow of membrane into tethers extracted from neuronal growth cones, Biophys. J. 70 (1996) 358–369.
[20] R.M. Hochmuth, W.D. Marcus, Membrane tethers formed from blood cells with available area and determination of their adhesion energy, Biophys. J. 82 (2002) 2964–2969.
[21] S. Steltenkamp, C. Rommel, J. Wegener, A. Janshoff, Membrane stiffness of animal cells challenged by osmotic stress, Small 2 (2006) 1016–1020.
[22] M.P. Sheetz, Cell control by membrane–cytoskeleton adhesion, Nat. Rev. Mol. Cell Biol. 2 (2001) 392–396.
[23] A.M. Woodward, D.H. Crouch, Cellular distributions of the ERM proteins in MDCK epithelial cells: regulation by growth and cytoskeletal integrity, Cell Biol. Int. 25 (2001) 205–213.
[24] W. Rawicz, K.C. Olbrich, T. McIntosh, D. Needham, E. Evans, Effect of chain length and unsaturation on elasticity of lipid bilayers, Biophys. J. 79 (2000) 328–339.
[25] M. Algrain, O. Turunen, A. Vaheri, D. Louvard, M. Arpin, Ezrin contains cytoskeleton and membrane binding domains accounting for its proposed role as a membrane-cytoskeletal linker, J. Cell Biol. 120 (1993) 129–139.
[26] M. Berryman, Z. Franck, A. Bretscher, Ezrin is concentrated in the apical microvilli of a wide variety of epithelial cells whereas moesin is found primarily in endothelial cells, J. Cell Sci. 105 (1993) 1025–1043.
[27] U. Komaragiri, M.R. Begley, J.G. Simmonds, The mechanical response of freestanding circular elastic films under point and pressure loads, J. Appl. Mech. 72 (2005) 203–212.
[28] C. Lee, X. Wei, J.W. Kysar, J. Hone, Measurement of the elastic properties and intrinsic strength of monolayer graphene, Science 321 (2008) 385–388.
[29] M. Radmacher, Measuring the elastic properties of biological samples with the AFM, IEEE Eng. Med. Biol. Mag. 16 (1997) 47–57.
[30] A.B. Mathur, A.M. Collinsworth, W.M. Reichert, W.E. Kraus, G.A. Truskey, Endothelial, cardiac muscle and skeletal muscle exhibit different viscous and elastic properties as determined by atomic force microscopy, J. Biomech. 34 (2001) 1545–1553.
[31] K.D. Costa, F.C.P. Yin, Analysis of indentation: implications for measuring mechanical properties with atomic force microscopy, J. Biomech. Eng. 121 (1999) 462–471.
[32] B.J. Briscoe, K.S. Sebastian, M.J. Adams, The effect of indenter geometry on the elastic response to indentation, J. Phys. D Appl. Phys. 27 (1994) 1156.
[33] D.C. Lin, E.K. Dimitriadis, F. Horkay, Robust strategies for automated AFM force curve analysis—II: adhesion-influenced indentation of soft, elastic materials, J. Biomech. Eng. 129 (2007) 904–912.
[34] K.W. Hunter, Ezrin, a key component in tumor metastasis, Trends Mol. Med. 10 (2004) 201–204.
[35] F. Guilak, G.R. Erickson, H.P. Ting-Beall, The effects of osmotic stress on the viscoelastic and physical properties of articular chondrocytes, Biophys. J. 82 (2002) 720–727.
[36] C. Spagnoli, A. Beyder, S. Besch, F. Sachs, Atomic force microscopy analysis of cell volume regulation, Phys. Rev. E 78 (2008) 031916.

[37] M. Kiesel, R. Reuss, J. Endter, D. Zimmermann, H. Zimmermann, R. Shirakashi, E. Bamberg, U. Zimmermann, V.L. Sukhorukov, Swelling-activated pathways in human T-lymphocytes studied by cell volumetry and electrorotation, Biophys. J. 90 (2006) 4720–4729.
[38] H. Ting-Beall, D. Needham, R. Hochmuth, Volume and osmotic properties of human neutrophils, Blood 81 (1993) 2774–2780.
[39] F. Brochard-Wyart, N. Borghi, D. Cuvelier, P. Nassoy, Hydrodynamic narrowing of tubes extruded from cells, Proc. Natl. Acad. Sci. 103 (2006) 7660–7663.
[40] M. Krieg, J. Helenius, C.P. Heisenberg, D.J. Muller, A bond for a lifetime: employing membrane nanotubes from living cells to determine receptor-ligand kinetics, Angew. Chem. Int. Ed. 47 (2008) 9775–9777.